

Predictors for Functionally Significant In-Stent Restenosis

An Integrated Analysis Using Coronary Angiography, IVUS, and Myocardial Perfusion Imaging

Soo-Jin Kang, MD, PhD,* Young-Rak Cho, MD,† Gyung-Min Park, MD,*
Jung-Min Ahn, MD,* Seung-Bong Han, PhD,‡ Jong-Young Lee, MD,*
Won-Jang Kim, MD,* Duk-Woo Park, MD, PhD,‡ Seung-Whan Lee, MD, PhD,*
Young-Hak Kim, MD, PhD,* Cheol Whan Lee, MD, PhD,* Seong-Wook Park, MD, PhD,*
Gary S. Mintz, MD,§ Seung-Jung Park, MD, PhD*
Seoul, South Korea; and New York, New York

OBJECTIVES The aim of this study was to assess the clinical and morphological predictors for functionally significant in-stent restenosis (ISR).

BACKGROUND Although they have been studied de novo in native coronary artery lesions, the relationships between clinical and morphological characteristics and the hemodynamic significance of ISR are not well understood.

METHODS In 175 patients with ISR of a single coronary artery (angiographic stenosis >50%), we compared quantitative coronary angiography and intravascular ultrasound (IVUS) with stress myocardial single-photon emission computed tomography (SPECT). A positive SPECT was a reversible perfusion defect in the territory of the ISR artery.

RESULTS Overall, 103 (59%) patients had a positive SPECT. In-segment IVUS minimal lumen area (MLA) was significantly smaller in lesions with positive SPECT compared with negative SPECT ($1.7 \pm 0.5 \text{ mm}^2$ vs. $2.4 \pm 0.8 \text{ mm}^2$, $p < 0.001$). Stent underexpansion (minimal stent area $< 5.0 \text{ mm}^2$) was more common in the positive SPECT group than in the negative SPECT group (52% vs. 32%, $p = 0.010$). A positive SPECT was seen in 54% (65 of 121) of focal ISR lesions compared with 70% (38 of 54) of multifocal or diffuse ISR lesions as assessed by IVUS ($p = 0.039$). Independent determinants for a positive SPECT were diabetes (odds ratio [OR]: 2.41; 95% confidence interval [CI]: 1.02 to 5.68; $p = 0.046$), in-segment angiographic diameter stenosis (OR: 1.06; 95% CI: 1.03 to 1.09; $p < 0.001$), in-segment IVUS-MLA (OR: 0.30; 95% CI: 0.14 to 0.63; $p = 0.001$), stent underexpansion (minimal stent area $< 5.0 \text{ mm}^2$), (OR: 2.91; 95% CI: 1.19 to 7.07; $p = 0.019$), proximal location of the IVUS-MLA (OR: 4.62; 95% CI: 1.75 to 12.18; $p = 0.002$), and a multifocal or diffuse ISR pattern (OR: 2.50; 95% CI: 0.99 to 6.28; $p = 0.050$). An in-segment angiographic diameter stenosis $\geq 69.5\%$ (72% sensitivity, 74% specificity, area under the curve = 0.793) and an IVUS-MLA $\leq 1.9 \text{ mm}^2$ (67% sensitivity, 75% specificity, area under the curve = 0.756) best predicted a positive SPECT; however, the overall diagnostic accuracies were only 73% and 70%, respectively.

CONCLUSIONS In lesions with ISR, neither angiography nor IVUS accurately predicted an abnormal SPECT. (J Am Coll Cardiol Img 2013;6:1183–90) © 2013 by the American College of Cardiology Foundation

The clinical decision whether to treat coronary artery in-stent restenosis (ISR) should be based on symptoms and objective evidence of ischemia (1–3). In native coronary artery stenoses, the angiographic and intravascular ultrasound (IVUS) predictors for ischemia have been reported (4–6). However, there are few studies showing the relationship between the clinical and morphological features of ISR and its hemodynamic significance. Thus, we performed an integrated analysis of quantitative coronary angiography, IVUS, and myocardial perfusion imaging to assess the clinical and anatomic factors determining the functional significance of an ISR lesion in patients with single-vessel disease.

METHODS

ABBREVIATIONS AND ACRONYMS

CI	= confidence interval
DS	= diameter stenosis
IH	= intimal hyperplasia
%IH	= percentage of intimal hyperplasia
ISR	= in-stent restenosis
IVUS	= intravascular ultrasound
MLA	= minimal lumen area
MLD	= minimal lumen diameter
NPV	= negative predictive value
OR	= odds ratio
PPV	= positive predictive value
SPECT	= single-photon emission computed tomography

Study population. Between January 2007 and December 2011, 290 patients with an ISR lesion within the proximal or mid segment of a single epicardial coronary artery underwent both IVUS and stress myocardial single-photon emission computed tomography (SPECT). Exclusion criteria were the presence of 2- or 3-vessel disease (i.e., a stenosis in another vessel) or multiple stenoses (angiographic stenosis [diameter stenosis (DS)] >50% on visual estimation) within the target vessel that would complicate the interpretation of the SPECT images, the presence of a bypass graft, ISR within a side branch, acute myocardial infarction, scarred myocardium or regional wall motion abnormality, left ventricular ejection fraction <50%, left

main coronary artery stenosis >30%, the presence of a fixed perfusion defect on SPECT, and cases in which the IVUS imaging catheter failed to cross the ISR lesion. ISR lesions with total occlusion were excluded except in 4 patients in whom guidewire passage restored coronary flow, and IVUS examination could be completed. Thus, a total of 175 patients with a single ISR lesion and no other coronary stenosis were included in the current analysis. Treatment of ISR lesions was at the operators' discretion

and was determined after evaluating both clinical and lesion-specific data.

Angiographic analysis. Quantitative coronary angiography was performed using standard techniques with automated edge-detection algorithms (CAAS-5, Pie Medical, Maastricht, the Netherlands) in the angiographic analysis center of the CardioVascular Research Foundation, Seoul, South Korea. Angiographic restenosis was defined as DS >50% at follow-up angiography and classified as suggested by Mehran et al. (7). The minimal lumen diameter (MLD) was measured within the stent (in-stent), within the 5-mm-long proximal and distal segments adjacent to the edges of the stent, and within the segment that included the proximal and distal 5-mm-long reference segments as well as the stent (in-segment).

IVUS imaging and analysis. After intracoronary administration of 0.2 mg nitroglycerin, IVUS imaging was performed using motorized transducer pullback (0.5 mm/s) and a commercial scanner (Boston Scientific/SCIMED, Minneapolis, Minnesota) with a rotating, 40-MHz transducer within a 3.2-F imaging sheath. Using computerized planimetry (EchoPlaque 3.0, Indec Systems, Mountain View, California), offline quantitative IVUS analysis was performed in a core laboratory at the Asan Medical Center. In-stent measurements were obtained every 1 mm and included the external elastic membrane, stent, lumen (intrastent lumen bounded by the borders of the stent and intimal hyperplasia [IH]), and IH (stent minus intrastent lumen) areas. The percentage of IH (%IH) was defined as the IH area divided by the stent area. Volumes were calculated using Simpson's rule and then normalized for analysis length (normalized volume). Stent underexpansion was defined as minimal stent area <5 mm² (8,9). The external elastic membrane and the smallest lumen areas were measured within the 5-mm-long reference segments proximal and distal to the stent edges. In parallel with angiographic measurements, both in-stent and in-segment (stent plus 5-mm-long reference segment) minimum lumen areas (MLAs) were identified and measured. According to the longitudinal distribution of significant IH assessed by IVUS, ISR patterns were classified as follows: 1) focal

From the *Department of Cardiology, University of Ulsan College of Medicine, Asan Medical Center, Seoul, South Korea; †Department of Cardiology, Dong-A University Hospital, Pusan, Korea; ‡Department of Biostatistics, University of Ulsan College of Medicine, Asan Medical Center, Seoul, South Korea; and the §Cardiovascular Research Foundation, New York, New York. This study was supported by a grant from the Korea Healthcare Technology Research and Development Project, Ministry of Health and Welfare (A120711), and CardioVascular Research Foundation, Seoul, South Korea. Dr. Mintz has received grant support from BostonScientific, Volcano, and InfraReDx; and is a consultant or speaker for BostonScientific, Volcano, St. Jude, and InfraReDx. All other authors have reported that they have no relationships relevant to the contents of this paper to disclose. Stephen Nicholls, MBBS, PhD, served as Guest Editor for this article.

ISR was defined as %IH >50% and ≤ 10 mm in length; 2) multifocal ISR contained multiple focal areas of ISR; and 3) diffuse ISR was defined as %IH >50% and >10 mm in length.

Stent malapposition was defined as separation of at least 1 stent strut not in contact with the intimal surface of the vessel wall that was not overlapping a side branch with evidence of blood speckling behind the strut (8).

Myocardial perfusion imaging. Gated thallous chloride (Tl-201) SPECT images were acquired after adenosine stress testing (post-stress SPECT) and again 4 h after the injection of Tl-201 chloride (redistribution SPECT). Patients abstained from caffeine-containing foods and beverages and drugs such as aminophylline and theophylline 24 h before the test. Adenosine was intravenously administered at a rate of 140 $\mu\text{g}/\text{kg}/\text{min}$ for 6 min. Three minutes after the initiation of the adenosine infusion, a dose of Tl-201 (range, 92.5 to 148 MBq, as determined by the subject's body weight) was injected intravenously. Six minutes after adenosine infusion, post-stress myocardial perfusion images were acquired with a 2-head gamma camera (Ecam, Siemens, Munich, Germany) equipped with low-energy all-purpose collimators (64×64 matrix, 32 projections over 180 degrees, 8 frames per cardiac cycle, 50 s per projection). A zoom factor of 1.78 was used. The pixel size was 5.4 mm. Transaxial slices were reconstructed with a Butterworth filter (order 5; cutoff frequency, 0.35). No attenuation or scatter correction was applied. Stress and rest tomographic images were displayed side by side in the short-axis, horizontal long-axis, and vertical long-axis reconstruction panels.

A 16-segment model was used in which myocardial segments were allocated to the territories of the different coronary arteries, as previously described (10,11). Apical segments were counted as defects only when contiguous with adjacent abnormal myocardial segments. Each vascular territory was classified as showing no perfusion defect if all segments in the territory had normal quantitative uptake. A vascular territory was considered a perfusion defect if quantitative tracer uptake in any segment within the vascular territory on the stress image was <75%. Each territory with a perfusion defect was further classified as reversible if any of the segments with a stress defect quantitatively improved tracer uptake on the image at rest or fixed if any of the segments with a stress defect showed no change or a further decrease in tracer uptake on the image at rest. Lesions with a fixed perfusion defect were excluded in the analysis. Accordingly, the result was

considered positive (positive SPECT) when a reversible perfusion defect or negative (negative SPECT) when a no perfusion defect was allocated to the perfusion territory of the target coronary artery (12).

Statistical analysis. All statistical analyses were performed using SPSS software (version 10.0, SPSS Inc., Chicago, Illinois). Continuous variables were expressed as mean \pm 1 SD or median and interquartile range and compared using an unpaired Student *t* test or the nonparametric Mann-Whitney test. Categorical variables were presented as counts and percentages and compared using chi-square statistics or the Fisher exact test.

Receiver-operating characteristic curves were analyzed to assess the best cutoff values of the angiographic and IVUS parameters to predict positive SPECT with maximal accuracy and using MedCalc Software (MedCalc Software, Mariakerke, Belgium). The optimal cutoff was calculated using the Youden index. The sensitivity, specificity, positive predictive value (PPV), and negative predictive value (NPV) with their 95% confidence interval (CI) were determined. Binary logistic regression analysis was performed to identify the independent determinants of positive SPECT. Candidate variables with a *p* value <0.2 on univariate analysis were included in multivariable model. The final models were determined by a backward variable selection approach in which the least significant variable was removed one by one after fitting a full model with the candidate variables. A *p* value <0.05 was considered statistically significant.

RESULTS

Baseline characteristics. The clinical characteristics of the 103 patients with a positive SPECT and the 72 patients with a negative SPECT were compared in Table 1. There was no difference in total stent length or duration since stent implantation between the 2 groups. A positive SPECT was more frequent in diabetic patients than in nondiabetic patients (70% vs. 51%, *p* = 0.010). There was no significant difference in the frequency of a positive SPECT between bare metal and drug-eluting ISR lesions (71% vs. 56%, *p* = 0.091). Additionally, the frequency of a positive SPECT was not different among the vessels (60% in the left anterior descending artery, 62% in the left circumflex artery, and 53% in the right coronary artery; *p* = 0.727).

Quantitative coronary angiographic data. Compared with ISR lesions with a negative SPECT, ISR lesions with a positive SPECT had a smaller in-stent and in-segment minimal lumen diameter

Table 1. Baseline Clinical Characteristics

	Thallium Positive (n = 103)	Thallium Negative (n = 72)	p Value
Age, yrs	62 (55–70)	64 (57–70)	0.607
Male	75 (73)	53 (74)	0.907
Diabetes	50 (49)	21 (29)	0.010
Hypertension	66 (64)	40 (56)	0.256
Smoking	45 (44)	40 (56)	0.122
Hyperlipidemia	79 (77)	54 (75)	0.796
Previous PCI	22 (21)	9 (13)	0.131
Renal failure	7 (7)	1 (1)	0.092
Ejection fraction, %	60.0 (55.0–63.0)	60.0 (59.0–63.5)	0.052
Clinical manifestation			
Asymptomatic	23 (22)	32 (44)	
Stable angina	51 (50)	24 (34)	0.678
Unstable angina	29 (28)	16 (22)	
No. of stents	1.0 (1.0–2.0)	1.0 (1.0–2.0)	0.151
Stent length, mm	31.2 (23.1–44.6)	29.0 (19.6–43.2)	0.283
Stent types			
Bare metal	25 (24)	10 (14)	0.091
Drug eluting	78 (76)	62 (86)	
Follow-up duration, mo	36.6 (15.7–74.4)	27.7 (8.9–57.8)	0.175
Values are median (interquartile range) compared by Mann-Whitney test, or n (%). PCI = percutaneous coronary intervention.			

(MLD) and a greater in-stent and in-segment DS (Table 2). Lesions with a positive SPECT also had a smaller MLD and a greater DS within the proximal 5-mm-long reference segments and more frequent proximal edge restenosis (23% vs. 10%, $p = 0.021$). Finally, a positive SPECT study for ischemia was more frequently seen in ISR lesions with a proliferative or total occlusion type of ISR compared with lesions with other more focal patterns of ISR (86% [18 of 21] vs. 55% [85 of 154], $p = 0.008$).

On receiver-operating characteristic curve analysis, an in-segment angiographic DS $\geq 69.5\%$ best predicted a positive SPECT with 72% sensitivity, 74% specificity, a PPV of 80%, and an NPV of 65% (area under the curve [AUC] = 0.793; 95% CI: 0.725 to 0.850, $p < 0.001$). The overall diagnostic accuracy was 73% (Fig. 1).

There was no difference in in-segment MLD (1.0 ± 0.5 mm vs. 1.0 ± 0.5 mm) or in-segment DS ($69.2 \pm 16.2\%$ vs. $68.6 \pm 16.5\%$) or angiographic restenosis pattern between diabetic and nondiabetic patients (all p values >0.05).

IVUS findings. Within both the proximal and distal reference segments, a smaller lumen area and a larger plaque burden were more frequently seen in

ISR lesions with a positive SPECT than in those with a negative SPECT (Table 2). Compared with the negative SPECT group, ISR lesions with positive SPECT showed a smaller in-stent MLA and normalized in-stent lumen volume and a greater %IH at the MLA site. In-segment MLA was significantly smaller in lesions with a positive SPECT compared with a negative SPECT (1.7 ± 0.5 mm² vs. 2.4 ± 0.8 mm², $p < 0.001$). Stent underexpansion (minimal stent area <5.0 mm²) was more common in the positive SPECT group than in the negative SPECT group (52% vs. 32%, $p = 0.010$). Conversely, there was no significant difference in the stent vessel wall malapposition rate between the 2 groups (8% vs. 3%, $p = 0.162$).

A positive SPECT was more frequent in ISR lesions in which the MLA site was located within the proximal one-third of the stented segment compared with the mid one-third or the distal one-third (80% vs. 54% vs. 42%, $p < 0.001$). A positive SPECT was seen in 54% (65 of 121) of focal ISR lesions versus 70% (38 of 54) of multifocal or diffuse ISR lesions as assessed by IVUS ($p = 0.039$).

On receiver-operating characteristic curve analysis, an in-segment MLA ≤ 1.9 mm² was the best cutoff value that predicted a positive SPECT with 67% sensitivity, 75% specificity, a PPV of 79%, and an NPV of 61% (AUC = 0.756, 95% CI: 0.685 to 0.818, $p = 0.001$). The overall diagnostic accuracy was 70% (Fig. 1). Furthermore, there was no difference in the in-segment MLA cutoff between bare metal stent (1.9 mm², AUC = 0.756) and the drug-eluting stent (1.9 mm², AUC = 0.753) subgroups.

There was no difference in the average reference lumen area between diabetic and nondiabetic patients (4.6 ± 2.2 mm² vs. 4.6 ± 2.0 mm²), in-segment MLA (2.0 ± 0.7 mm² vs. 1.9 ± 0.7 mm²), %IH ($64.9 \pm 20.4\%$ vs. $66.4 \pm 18.6\%$), or minimal stent area (5.3 ± 1.6 mm² vs. 5.6 ± 1.7 mm²) (all p values >0.05).

Independent determinants of a positive SPECT. The independent factors associated with a positive SPECT were diabetes, angiographic in-segment DS, IVUS in-segment MLA, stent underexpansion (minimal stent area <5.0 mm²), location of the IVUS-MLA site, and an IVUS multifocal or diffuse pattern of ISR (C-statistic = 0.879) (Table 3).

Treatment of ISR. Repeat revascularization was performed in 96 patients (93%) with a positive SPECT and 38 (53%) with a negative SPECT. Among the treated patients, despite the negative SPECT, 6 patients were asymptomatic, and the remaining 32 patients had angina symptoms at the time of ISR detection. Overall, 36 lesions (95%)

had an angiographic DS >70%, and all had an IVUS MLA <4.0 mm².

DISCUSSION

The major findings of this study were the following: 1) even in patients with angiographic ISR (DS >50%), 41% showed no ischemia as assessed by SPECT imaging; 2) the independent determinants of a positive SPECT were diabetes, severity of the angiographic DS, a smaller IVUS-MLA, proximal location of the IVUS-MLA, stent underexpansion, and multifocal or diffuse patterns of ISR assessed by IVUS; 3) an in-segment angiographic DS ≥69.5% and an IVUS-MLA ≤1.9 mm² best predicted a positive SPECT, although the overall diagnostic accuracy was only 73% and 70%, respectively. This was similar in bare metal and drug-eluting ISR lesions.

Previous data reported that ischemia-guided treatment of ISR lesions led to favorable clinical outcomes (13,14). However, as has been shown in many studies, coronary angiography often underestimated or overestimated the functional severity of de novo lesions (1,2,4,5,15), and visual-functional mismatches were encountered in as many as 40% of de novo native coronary lesions (6,16). Approximately half of patients with angiographic ISR have been reported to be asymptomatic (17,18). In our current study, 41% of the ISR lesions with an angiographic DS >50% and 20% of the ISR lesions with an angiographic DS >70% were not associated with ischemia, as shown by a negative SPECT study. When operator decision making is based on the angiographic findings alone, those patients without functionally significant ISR may undergo unnecessary clinically driven repeat revascularization, as has been shown in randomized trials with both angiographic and clinical follow-up (19). Our current data expanded previous observations that routine angiographic follow-up led to an oculostenotic reflex and increasing target lesion and target vessel revascularization rates compared with clinical follow-up alone (19).

Previous studies provided limited information regarding patients with ISR lesions that were more likely to be functionally significant and cause ischemia. Nam et al. (14) reported that angiographic MLD, DS, and lesion length are related to a fractional flow reserve <0.80 in ISR lesions. Koch et al. (20) reported that the independent predictors of a reversible perfusion defect on SPECT imaging are the angiographic DS and a resting perfusion defect. Even though ISR lesions tended to be less complex and less eccentric, previous studies did not support

Table 2. Quantitative Angiographic and IVUS Findings

	Thallium Positive (n = 103)	Thallium Negative (n = 72)	p Value
Angiographic data			
Proximal reference MLD, mm	2.4 (1.3–3.0)	2.7 (2.4–3.1)	0.016
Proximal reference DS, %	24.0 (13.0–61.0)	17.0 (7.8–27.0)	0.001
Distal reference MLD, mm	2.0 (1.7–2.4)	2.1 (1.7–2.5)	0.179
Distal reference DS, %	22.0 (13.0–34.0)	21.0 (12.0–39.0)	0.931
In-stent MLD, mm	0.9 (0.6–1.3)	1.5 (1.1–1.9)	<0.001
In-stent DS, %	73.0 (56.0–84.0)	53.5 (39.3–62.0)	<0.001
In-segment MLD, mm	0.7 (0.5–1.1)	1.3 (0.9–1.6)	<0.001
In-segment DS, %	0.7 (0.5–1.1)	57.0 (51.0–70.0)	<0.001
Restenosis pattern			
Marginal	17 (16)	18 (25)	
Focal body	47 (46)	35 (49)	
Multifocal	5 (5)	4 (5)	0.138
Diffuse in-stent	16 (15)	12 (17)	
Proliferative	14 (14)	3 (4)	
Total occlusion	4 (4)	0 (0)	
IVUS data			
Proximal reference segment			
Lumen area, mm ²	4.4 (2.3–7.1)	6.4 (5.1–8.3)	<0.001
EEM area, mm ²	14.1 (11.5–18.1)	14.9 (12.5–18.8)	0.353
Plaque burden, %	66.3 (57.5–80.7)	55.5 (46.1–62.7)	<0.001
Distal reference segment			
Lumen area, mm ²	3.0 (2.0–4.1)	4.1 (2.8–5.7)	0.001
EEM area, mm ²	7.8 (5.7–10.3)	9.0 (6.1–13.3)	0.080
Plaque burden, %	60.9 (47.4–71.9)	52.9 (38.9–69.0)	0.027
In-stent segment			
MLA within stent, mm ²	1.7 (1.3–2.2)	2.4 (1.9–3.3)	<0.001
EEM area at the MLA site, mm ²	14.6 (11.8–18.0)	13.5 (10.8–18.2)	0.284
Stent area at the MLA site, mm ²	7.0 (5.3–8.6)	6.8 (5.4–8.3)	0.952
%IH at the MLA site, %	74.6 (63.3–82.2)	63.1 (52.7–73.3)	<0.001
Minimal stent area, mm ²	5.0 (4.1–6.3)	5.8 (4.7–6.8)	0.034
In-stent volumetric data			
Normalized lumen volume, mm ²	4.5 (3.8–5.6)	5.3 (4.0–6.5)	0.016
Normalized EEM volume, mm ²	14.4 (12.2–17.4)	14.6 (12.8–17.4)	0.446
Normalized stent volume, mm ²	7.0 (5.6–8.2)	7.7 (6.1–8.9)	0.039
Normalized IH volume, mm ²	1.9 (1.2–3.6)	1.9 (1.3–2.8)	0.985
%IH volume, mm ²	(18.7–46.5)	26.1 (16.0–39.4)	0.309
IVUS-defined ISR pattern			
Focal	65 (63)	56 (78)	
Multifocal	18 (18)	6 (8)	0.080
Diffuse	20 (19)	10 (14)	

Values are median (interquartile range), compared by Mann-Whitney test, or n (%).
 DS = diameter of stenosis; EEM = external elastic membrane; IH = intimal hyperplasia; %IH = percentage of intimal hyperplasia; ISR = in-stent restenosis; IVUS = intravascular ultrasound; MLA = minimal lumen area; MLD = minimal lumen diameter.

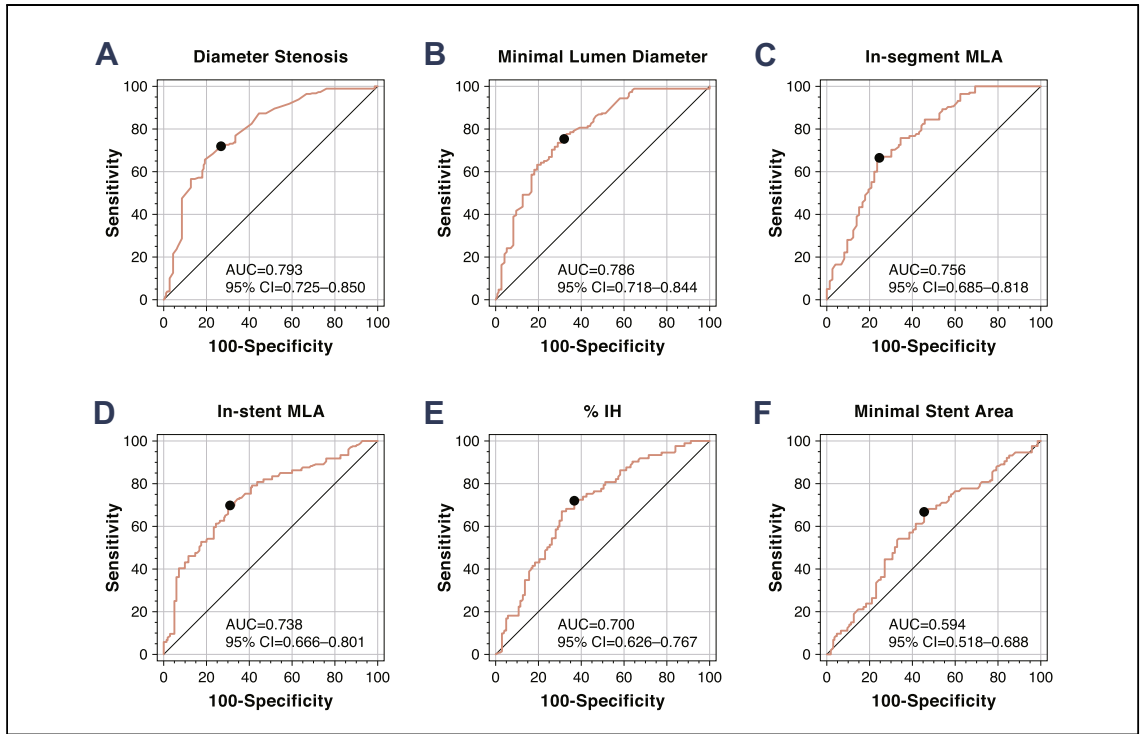


Figure 1. Receiver-Operating Characteristic Curve Analysis for the Prediction of a Positive SPECT

(A) An in-segment angiographic diameter stenosis $\geq 69.5\%$ best predicted a positive SPECT (72% sensitivity, 74% specificity, 80% PPV, 65% NPV). (B) The cutoff of in-segment minimal lumen diameter was ≤ 1.1 mm (77% sensitivity, 68% specificity, 78% PPV, 67% NPV). (C) An in-segment minimal lumen area (MLA) ≤ 1.9 mm² was the best cutoff value to predict a positive SPECT (67% sensitivity, 75% specificity, 79% PPV, 61% NPV). (D) The cutoff of in-stent MLA was ≤ 2.1 mm² (69% sensitivity, 70% specificity, 62% PPV, 77% NPV). (E) The cutoff of %IH at the MLA site was $\geq 68\%$ (67% sensitivity, 69% specificity, 60% PPV, 75% NPV). (F) The cutoff of a minimal stent area was ≤ 5.1 mm² (67% sensitivity, 54% specificity, 51% PPV, 71% NPV). AUC = area under the curve; CI = confidence interval; %IH = percentage of intimal hyperplasia; MLA = minimal lumen area; NPV = negative predictive value; PPV = positive predictive value; SPECT = single-photon emission computed tomography.

the hypothesis that greater angiographic DS severity was necessary to create ischemia compared with de novo native coronary lesions (20–22). The threshold of the angiographic DS causing reversible perfusion defects was found to be similar between ISR (53%,

AUC = 0.63) and de novo native coronary lesions (53%, AUC = 0.61) (20). Similarly, compared with a fractional flow reserve < 0.75 , the cutoff value of the angiographic DS was 57% for de novo native coronary lesions (80% sensitivity, 83% specificity) and 55% for ISR lesions (81% sensitivity, 81% specificity) (22). Our current study showed that an in-segment angiographic DS $\geq 69\%$ best predicted a positive SPECT (72% sensitivity, 74% specificity). Additionally, a positive SPECT was more frequently observed in lesions with a proliferative or total occlusion type of ISR compared with the lesions with other more focal patterns.

The current IVUS analysis expanded on these angiographic studies to show that more severe and extensive ISR lesions as well as lesions with stent underexpansion were more likely to be ischemia producing. The following IVUS parameters were related to ischemia: more severe reference segment disease, a smaller MLA, a greater %IH, stent underexpansion, an IVUS-MLA that was located in

Table 3. Multivariable Analysis for the Prediction of Positive SPECT

	OR	95% CI	p Value
Diabetes	2.41	1.02–5.68	0.046
In-segment DS	1.06	1.03–1.09	< 0.001
In-segment IVUS-MLA	0.30	0.14–0.63	0.001
Stent underexpansion	2.91	1.19–7.07	0.019
Proximal one-third location of the MLA	4.62	1.75–12.18	0.002
Multifocal or entirely diffuse stenosis	2.50	0.99–6.28	0.050

Multivariable analysis included diabetes, in-segment angiographic DS (%), in-segment minimal lumen diameter (mm), angiographic involvement of proximal edge, percentage of intimal hyperplasia, in-segment IVUS-MLA (mm²), MLA location at proximal one-third of the stent, stent underexpansion (minimal stent area < 5.0 mm²), in-stent normalized lumen volume (mm²), and multiple stenosis or entire diffuse in-stent restenosis.

CI = confidence interval; OR = odds ratio; SPECT = single-photon emission computed tomography; other abbreviations as in Table 2.

the proximal one-third of the stented segment, and a more severe semiquantitative pattern of ISR (multifocal or diffuse pattern). The best cutoff that predicted a positive SPECT was an IVUS in-segment MLA ≤ 1.9 mm²; this was similar to the previously reported MLA of ≤ 2.1 mm² that best predicted a positive SPECT in de novo native coronary lesions (12). However, with an overall diagnostic accuracy of only 70%, the IVUS-MLA did not improve on the ability of the angiographic DS to predict a positive SPECT. Anatomic lesion severity, regardless of the way in which it was assessed, was only one of the multiple determinants of ischemia, whether in de novo stenoses or in ISR lesions.

Although there was no difference in angiographic and IVUS lesion characteristics between diabetic and nondiabetic patients in the current study, diabetic patients more frequently had a positive SPECT for a given stenosis severity. Moreover, diabetes was the only clinical predictor of a positive SPECT. Previous data suggested that the impairment of endothelium-dependent vasodilation in the coronary microvasculature was associated with abnormal myocardial perfusion in diabetic patients (23–25).

Study limitations. To avoid false-negative SPECT from balanced ischemia, we included only patients with single-vessel ISR with no other stenosis. Therefore, the results could not be applied to

multivessel disease or left main coronary artery disease. Second, most of the ISR lesions with very tight stenosis or total occlusions were excluded due to the technical difficulty of an IVUS examination. Third, the optimal treatment strategies for restenotic lesions and long-term clinical outcomes were not evaluated. Fourth, a positive SPECT does not always mean ischemia, whereas a negative SPECT does not always exclude ischemia. SPECT has limitations such as scatter or attenuation artifacts and spatial resolution, and a positive SPECT reflects nonuniform distribution of the tracer and not necessarily myocardial ischemia. Finally, the impact of in-stent neointimal tissue characteristics (i.e., neoatherosclerosis) on hemodynamic significance was not assessed.

CONCLUSIONS

In ISR lesions, neither angiography nor IVUS accurately predicted the hemodynamic significance as assessed by SPECT imaging. Therefore, decision making for the treatment of ISR lesions should not be based on anatomic assessment alone.

Reprint requests and correspondence: Dr. Seung-Jung Park, Department of Cardiology, Asan Medical Center, 388-1 Poongnap-dong, Songpa-gu, Seoul, 138-736 South Korea. *E-mail:* sjpark@amc.seoul.kr.

REFERENCES

1. Tonino PA, Fearon WF, De Bruyne B, et al. Angiographic versus functional severity of coronary artery stenoses in the FAME study fractional flow reserve versus angiography in multivessel evaluation. *J Am Coll Cardiol* 2010;55:2816–21.
2. Tonino PA, De Bruyne B, Pijls NH, et al, for the FAME Study Investigators. Fractional flow reserve versus angiography for guiding percutaneous coronary intervention. *N Engl J Med* 2009;360:213–24.
3. Shaw LJ, Berman DS, Maron DJ, et al. Optimal medical therapy with or without percutaneous coronary intervention to reduce ischemic burden: results from the Clinical Outcomes Utilizing Revascularization and Aggressive Drug Evaluation (COURAGE) trial nuclear substudy. *Circulation* 2008;117:1283–91.
4. Kang SJ, Lee JY, Ahn JM, et al. Validation of intravascular ultrasound-derived parameters with fractional flow reserve for assessment of coronary stenosis severity. *Circ Cardiovasc Interv* 2011;4:65–71.
5. Ben-Dor I, Torguson R, Deksissa T, et al. Intravascular ultrasound lumen area parameters for assessment of physiological ischemia by fractional flow reserve in intermediate coronary artery stenosis. *Cardiovasc Revasc Med* 2012;13:177–82.
6. Park SJ, Kang SJ, Ahn JM, et al. Visual-functional mismatch between coronary angiography and fractional flow reserve. *J Am Coll Cardiol Intv* 2012;5:1029–36.
7. Mehran R, Dangas G, Abizaid AS, et al. Angiographic patterns of in-stent restenosis: classification and implications for long-term outcome. *Circulation* 1999;100:1872–8.
8. Mintz GS, Nissen SE, Anderson WD, et al. American College of Cardiology Clinical Expert Consensus Document on Standards for Acquisition, Measurement and Reporting of Intravascular Ultrasound Studies (IVUS). A report of the American College of Cardiology Task Force on Clinical Expert Consensus Documents. *J Am Coll Cardiol* 2001;37:1478–92.
9. Sonoda S, Morino Y, Ako J, et al. Impact of final stent dimensions on long-term results following sirolimus-eluting stent implantation: serial intravascular ultrasound analysis from the SIRIUS trial. *J Am Coll Cardiol* 2004;43:1959–63.
10. Cerqueira MD, Weissman NJ, Dilsizian V, et al. Standardized myocardial segmentation and nomenclature for tomographic imaging of the heart: a statement for healthcare professionals from the Cardiac Imaging Committee of the Council on Clinical Cardiology of the American Heart Association. *Circulation* 2002;105:539–42.
11. Hachamovitch R, Hayes SW, Friedman JD, Cohen I, Berman DS. Stress myocardial perfusion single-photon emission computed tomography is clinically effective and cost effective in risk stratification of patients with a high likelihood of coronary artery disease (CAD) but no known CAD. *J Am Coll Cardiol* 2004;43:200–8.

12. Ahn JM, Kang SJ, Mintz GS, et al. Validation of minimal luminal area measured by intravascular ultrasound for assessment of functionally significant coronary stenosis comparison with myocardial perfusion imaging. *J Am Coll Cardiol Intv* 2011;4:665-71.
13. Kruger S, Hoffmann R, Koch KC, et al. Use of fractional flow reserve versus stress perfusion scintigraphy in stent-restenosis. *Eur J Intern Med* 2005;16:429-31.
14. Nam CW, Rha SW, Koo BK, et al. Usefulness of coronary pressure measurement for functional evaluation of drug-eluting stent restenosis. *Am J Cardiol* 2011;107:1783-6.
15. Christou MA, Siontis GC, Katritsis DG, Ioannidis JP. Meta-analysis of fractional flow reserve versus quantitative coronary angiography and noninvasive imaging for evaluation of myocardial ischemia. *Am J Cardiol* 2007;99:450-6.
16. Kang SJ, Ahn JM, Song H, et al. Usefulness of minimal luminal coronary area determined by intravascular ultrasound to predict functional significance in stable and unstable angina pectoris. *Am J Cardiol* 2012;109:947-53.
17. Ruygrok PN, Webster MW, de Valk V, et al. Clinical and angiographic factors associated with asymptomatic restenosis after percutaneous coronary intervention. *Circulation* 2001;104:2289-94.
18. Hernandez RA, Macaya C, Iniguez A, et al. Midterm outcome of patients with asymptomatic restenosis after coronary balloon angioplasty. *J Am Coll Cardiol* 1992;19:1402-9.
19. Pinto DS, Stone GW, Ellis SG, et al. Impact of routine angiographic follow-up on the clinical benefits of paclitaxel-eluting stents: results from the TAXUS-IV trial. *J Am Coll Cardiol* 2006;48:32-6.
20. Koch KC, Schaefer WM, Ersahin K, et al. Haemodynamic significance of stent lesions compared to native coronary lesions: a myocardial perfusion imaging study. *Heart* 2004;90:691-2.
21. Hoffmann R, Mintz GS, Dussailant GR, et al. Patterns and mechanisms of stent restenosis: a serial intravascular ultrasound study. *Circulation* 1996;94:1247-54.
22. Krüger S, Koch KC, Kaumanns I, Merx MW, Hanrath P, Hoffmann R. Clinical significance of fractional flow reserve for evaluation of functional lesion severity in stent restenosis and native coronary arteries. *Chest* 2005;128:1645-9.
23. Marcus M, Chilian W, Kanatsuka H, Dellsperger KC, Eastham CL, Lamping KG. Understanding the coronary circulation through studies at the microvascular level. *Circulation* 1990;82:1-7.
24. Peix A, Cabrera LO, Heres F, et al. Interrelationship between myocardial perfusion imaging, coronary calcium score, and endothelial function in asymptomatic diabetics and controls. *J Nucl Cardiol* 2011;18:398-406.
25. Anand D, Lim E, Hopkins D, et al. Risk stratification in uncomplicated type 2 diabetes: prospective evaluation of the combined use of coronary artery calcium imaging and selective myocardial perfusion scintigraphy. *Eur Heart J* 2006;27:713-21.

Key Words: in-stent restenosis ■ intravascular ultrasound ■ myocardial perfusion imaging.